lyso-PAFAT and LPCAT activities of LPCAT2 (Fig. 2).

The activation of LPCAT2 in LPS-stimulated RAW264.7 cells was dependent on MK2 located in the downstream of p38 MAPK. Both p38α and p38δ are mainly expressed in macrophages (27), and p38α and p38β signals are inhibited by SB203580. Thus, Fig. 3 and 4 suggest an LPCAT2 phosphorylation mediated by p38α–MK2 axis. MK2 induces the phosphorylation of its substrates with the consensus sequence (Hyd-X-R-X-X-S) (12,22). Near the N-terminus of LPCAT2, ^{29}VPRQAS^{34} was detected as corresponding to the consensus sequence. Thus, MK2 may directly phosphorylate LPCAT2, although it is possible that other kinases are present to link the two proteins. Future determination of the three dimensional structure of LPCAT2 should definitively clarify this activation mechanism.

LPCAT2 has lyso-PAFAT and LPCAT activities, both of which are enhanced by LPS-stimulation. The endogenous LPCAT activity in RAW264.7 cells was much higher than its lyso-PAFAT activity (Fig. 2B and C). Thus, activated LPCAT2 may function as a lyso-PAFAT to produce PAF. It is also possible that the LPCAT activity of LPCAT2 plays an important role in the storage of phospholipid precursors of PAF and eicosanoids (1). LPCAT2 catalyzes the membrane biogenesis (LPCAT activity) of inflammatory cells, while producing PAF (lyso-PAFAT activity) in response to external stimuli. Further studies are needed to elucidate the physiological and pathological importance of these dual activities.

This is the first report on the posttranslational modification of lysophospholipid acyltransferases (LPLATs) functioning in Lands' cycle. Our results showed that LPCAT2, a member of LPLATs, can produce lipid mediator and may contribute to membrane dynamics in response to extracellular stimuli.

This study will aid in the development of new anti-inflammatory drugs that inhibit PAF production by exogenous insults while maintaining the constitutive levels of the mediator. Because of the physiologically important roles of PAF,

PAFR antagonists have encountered several adverse effects during drug development. Inhibition of inducible PAF production by phospho-LPCAT2, but not unphospho-LPCAT2 or LPCAT1 (constitutive lyso-PAFAT) could serve as a potential target of medical interventions. These findings improve our understanding of both inflammatory responses and membrane biogenesis.

ACKNOWLEDGEMENTS

We are grateful to Y. Gotoh, M. Nakamura, S. Ishii, Y. Kita, S.M. Tokuoka, D. Hishikawa, A. Koeberle, T. Takahashi, T. Harayama Y. Takahashi and all the members of our laboratory (The University of Tokyo) for their valuable suggestions; and to Dr. J.-i. Miyazaki (Osaka University) for supplying the expression vector pCXN2.

REFERENCES

1. Shimizu, T. (2009) *Annu Rev Pharmacol Toxicol* **49**, 123-150
2. Prescott, S. M., Zimmerman, G. A., and McIntyre, T. M. (1990) *J Biol Chem* **265**, 17381-17384
3. Wykle, R. L., Malone, B., and Snyder, F. (1980) *J Biol Chem* **255**, 10256-10260
4. Nieto, M. L., Velasco, S., and Sanchez Crespo, M. (1988) *J Biol Chem* **263**, 2217-2222
5. Nixon, A. B., O'Flaherty, J. T., Salyer, J. K., and Wykle, R. L. (1999) *J Biol Chem* **274**, 5469-5473
6. Shindou, H., Ishii, S., Yamamoto, M., Takeda, K., Akira, S., and Shimizu, T. (2005) *J Immunol* **175**, 1177-1183
7. Owen, J. S., Baker, P. R., O'Flaherty, J. T., Thomas, M. J., Samuel, M. P., Wooten, R. E., and Wykle, R. L. (2005) *Biochim Biophys Acta* **1733**, 120-129
8. Harayama, T., Shindou, H., Ogasawara, R., Suwabe, A., and Shimizu, T. (2008) *J Biol Chem* **283**, 11097-11106
9. Shindou, H., Hishikawa, D., Nakanishi, H., Harayama, T., Ishii, S., Taguchi, R., and

Shimizu, T. (2007) *J Biol Chem* **282**, 6532-6539

10. Ben-Levy, R., Leighton, I. A., Doza, Y. N., Attwood, P., Morrice, N., Marshall, C. J., and Cohen, P. (1995) *EMBO J* **14**, 5920-5930
11. Engel, K., Kotlyarov, A., and Gaestel, M. (1998) *EMBO J* **17**, 3363-3371
12. Gaestel, M. (2006) *Nat Rev Mol Cell Biol* **7**, 120-130
13. Kotlyarov, A., Neininger, A., Schubert, C., Eckert, R., Birchmeier, C., Volk, H. D., and Gaestel, M. (1999) *Nat Cell Biol* **1**, 94-97
14. Werz, O., Klemm, J., Samuelsson, B., and Radmark, O. (2000) *Proc Natl Acad Sci U S A* **97**, 5261-5266
15. Lasa, M., Mahtani, K. R., Finch, A., Brewer, G., Saklatvala, J., and Clark, A. R. (2000) *Mol Cell Biol* **20**, 4265-4274
16. Shindou, H., and Shimizu, T. (2009) *J Biol Chem* **284**, 1-5
17. Bradford, M. M. (1976) *Anal Biochem* **72**, 248-254
18. Hishikawa, D., Shindou, H., Kobayashi, S., Nakanishi, H., Taguchi, R., and Shimizu, T. (2008) *Proc Natl Acad Sci U S A* **105**, 2830-2835
19. Kinoshita, E., Kinoshita-Kikuta, E., Takiyama, K., and Koike, T. (2006) *Mol Cell Proteomics* **5**, 749-757
20. Katayama, H., Tabata, T., Ishihama, Y., Sato, T., Oda, Y., and Nagasu, T. (2004) *Rapid Commun Mass Spectrom* **18**, 2388-2394
21. Nakamura, T., Myint, K. T., and Oda, Y. (2010) *J Proteome Res* **9**, 1385-1391
22. Stokoe, D., Caudwell, B., Cohen, P. T., and Cohen, P. (1993) *Biochem J* **296 (Pt 3)**, 843-849
23. Cano, E., Doza, Y. N., Ben-Levy, R., Cohen, P., and Mahadevan, L. C. (1996) *Oncogene* **12**, 805-812
24. Anderson, D. R., Meyers, M. J., Vernier, W. F., Mahoney, M. W., Kurumbail, R. G., Caspers, N., Poda, G. I., Schindler, J. F., Reitz, D. B., and Mourey, R. J. (2007) *J Med Chem* **50**, 2647-2654

25. Smith, W. L., DeWitt, D. L., and Garavito, R. M. (2000) *Annu Rev Biochem* **69**, 145-182

26. Smith, W. L., and Langenbach, R. (2001) *J Clin Invest* **107**, 1491-1495

27. Hale, K. K., Trollinger, D., Rihanek, M., and Manthey, C. L. (1999) *J Immunol* **162**, 4246-4252

FOOTNOTES

*This work was supported in part by Grants-in-Aid from the Ministry of Education, Culture, Sports, Science, and Technology (MEXT) of Japan (T.S.) and the Global COE Program (The University of Tokyo) from the Japan Society for Promotion of Sciences (T.S.). T.S. and H.S. were supported by the Center for NanoBio Integration at The University of Tokyo. H.S. was supported by Health and Labour Sciences Research Grants (Research on Allergic Disease and Immunology) from the Ministry of Health, Labour and Welfare; by a Grant-in-Aid for Young Scientists (B) from the MEXT of Japan; and by grants of the Uehara Memorial Foundation and the Cell Science Research Foundation.

[5]The abbreviations used are: PAF, platelet-activating factor; LPS, lipopolysaccharide; PC, phosphatidylcholine; PLA_2, phospholipase A_2; lyso-PAFAT, acetyl-CoA:lyso-PAF acetyltransferase; LPC, lysophosphatidylcholine; PAFR, PAF receptor; TLR, Toll-like receptor; MyD88, myeloid differentiation primary response gene 88; TAK1, tumor growth factor-β activated protein kinase 1; p38 MAPK, p38 mitogen activated protein kinase; MK2, MAPK-activated protein kinase 2; LPLATs, lysophospholipid acyltransferases.

FIGURE LEGENDS

FIGURE 1. LPCAT2 activation and phosphorylation

RAW264.7 cells transfected with vector, FLAG-LPCAT1, or FLAG-LPCAT2 were stimulated with 100 ng/ml LPS for 30 min. (A) LPS enhanced the activity of LPCAT2, but not that of LPCAT1. Open bars and closed bars indicate vehicle or LPS-stimulation, respectively. Results are expressed as the mean + S.D. of an experiment performed in triplicate. Three independent experiments showed similar results. (B) Western blot analysis was performed after phos-tag SDS-PAGE. Only LPCAT2 showed the shifted-band with LPS-stimulation indicating its phosphorylation. (C) Alignment of LPCAT2 in various species. The newly identified phosphorylation site, Ser34, was well-conserved among mammals. The accession numbers of LPCAT2 are available in Methods. Statistical analyses were performed by analysis of variance and Tukey's multiple comparison test.

FIGURE 2. Site-directed mutagenesis of LPCAT2

RAW264.7 cells transfected with vector, wild-type (WT), S34A, or S34D were stimulated with 100 ng/ml LPS for 30 min. (A) In Phos-tag Western blot analysis, only WT with LPS-stimulation showed the shifted-band. The two mutants showed no shift. Lyso-PAFAT (B) and LPCAT (C) activities were measured. S34A and S34D did not show the activation, and the activity of S34D was already high without LPS. Open bars and closed bars indicate vehicle or LPS-stimulation, respectively. Results are expressed as the mean + S.D. of an experiment performed in triplicate. Four independent experiments were performed with similar results. Statistical analyses were performed by analysis of variance and Tukey's multiple comparison test.

FIGURE 3. Time course for LPCAT2 phosphorylation

Mouse thioglycolate-induced peritoneal macrophages were stimulated with 100 ng/ml LPS for indicated periods. Microsomal proteins (100,000 × *g* pellets for 60 min) were analyzed by Western blot. Phosphorylated LPCAT2 and MK2 were appeared within 15-30 min. Arrowheads indicate MK2 splice variants. Three independent experiments were performed with similar

results.

FIGURE 4. Signaling pathway for LPCAT2 phosphorylation

RAW264.7 cells transfected with LPCAT2 were preincubated with or without each inhibitor for 1 h and subsequently stimulated with 100 ng/ml LPS for 30 min. See also Fig. 5. Supernatants (9,000 × *g* for 10 min) were subjected to Western blot analysis. (A) 1 μM (5*Z*)-7-oxozeaenol, (B) 20 μM SB203580, and (C) MK2 inhibitor III abolished LPCAT2 phosphorylation. SB202474 is an inactive analogue of SB203580. Arrowheads indicate MK2 splice variants. Three independent experiments were performed with similar results.

FIGURE 5. MK2-dependent LPCAT2 phosphorylation

MK2-siRNA was transfected into RAW264.7 cells stably expressing WT LPCAT2. The levels of MK2 mRNA (A) and MK2 protein (B) were decreased in the MK2 knocked-down cells (MK2-KD). Levels of phopho-MK2 and phospho-LPCAT2 were lower in MK2-KD than in negative control cells (NC). (C and D) LPS-stimulation induced neither lyso-PAFAT nor LPCAT activation in MK2-KD. Arrowheads indicate MK2 splice variants. Open bars and closed bars indicate vehicle or LPS-stimulation, respectively. Results are expressed as the mean + S.D. of an experiment performed in triplicate. Five independent experiments were performed with similar results. Statistical analyses were performed by analysis of variance and Tukey's multiple comparison test.

FIGURE 6. A proposed scheme of the molecular mechanism underlying LPCAT2 activation

The results of the present study indicate that LPCAT2 phosphorylation under LPS-stimulation depends on the MyD88, TAK1, p38α, and MK2 signaling pathway. Ser34 is the only phosphorylated site of LPCAT2 that enhances its catalytic activities.

Fig. 1

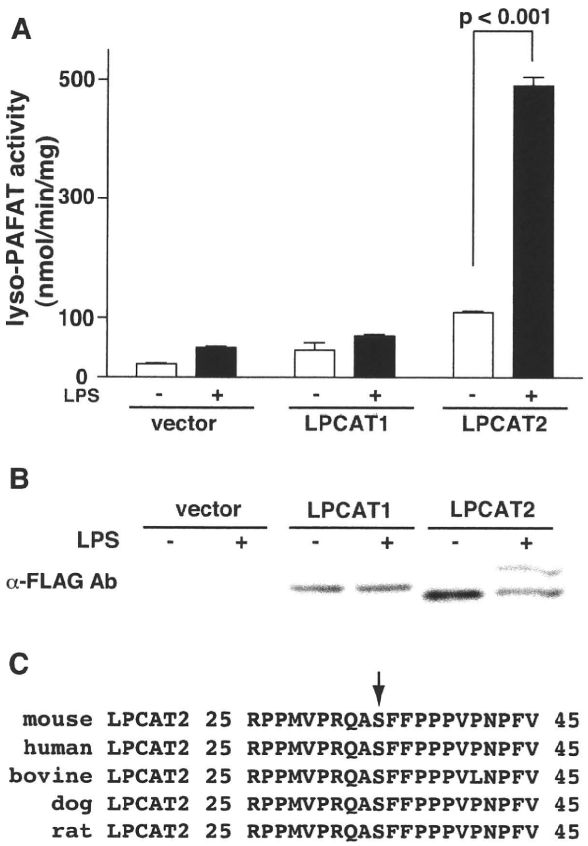

C

```
mouse LPCAT2 25 RPPMVPRQASFFPPPVPNPFV 45
human LPCAT2 25 RPPMVPRQASFFPPPVPNPFV 45
bovine LPCAT2 25 RPPMVPRQASFFPPPVLNPFV 45
dog LPCAT2 25 RPPMVPRQASFFPPPVPNPFV 45
rat LPCAT2 25 RPPMVPRQASFFPPPVPNPFV 45
```

Fig. 2

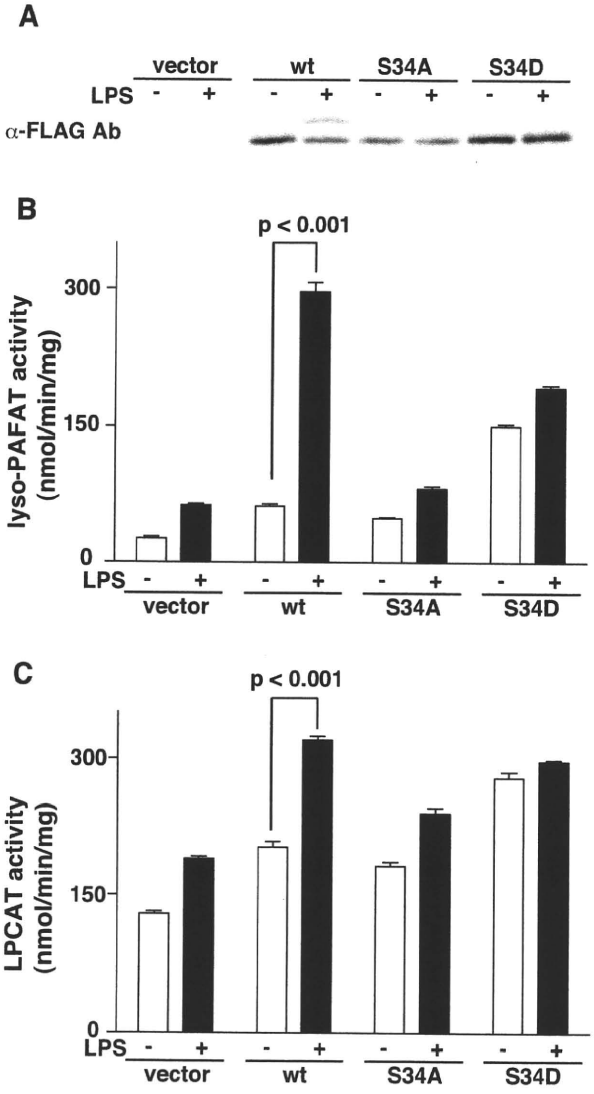
A
vector
wt
S34A
S34D
LPS - + - + - + - +
α-FLAG Ab
B
p < 0.001
lyso-PAFAT activity (nmol/min/mg)
300
150
0
LPS - + - + - + - +
vector
wt
S34A
S34D
C
p < 0.001
LPCAT activity (nmol/min/mg)
300
150
0
LPS - + - + - + - +
vector
wt
S34A
S34D

Fig. 3

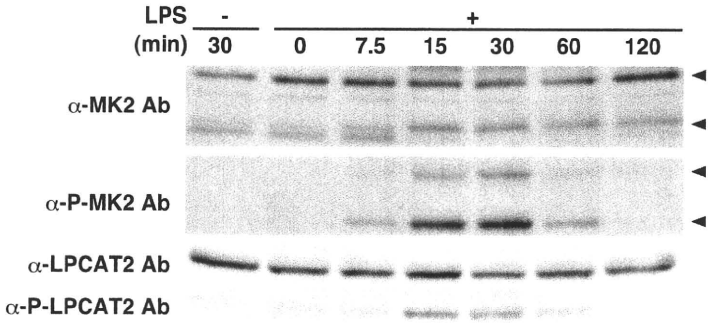
LPS
-
+
(min)
30
0
7.5
15
30
60
120
α-MK2 Ab
α-P-MK2 Ab
α-LPCAT2 Ab
α-P-LPCAT2 Ab

Fig. 4

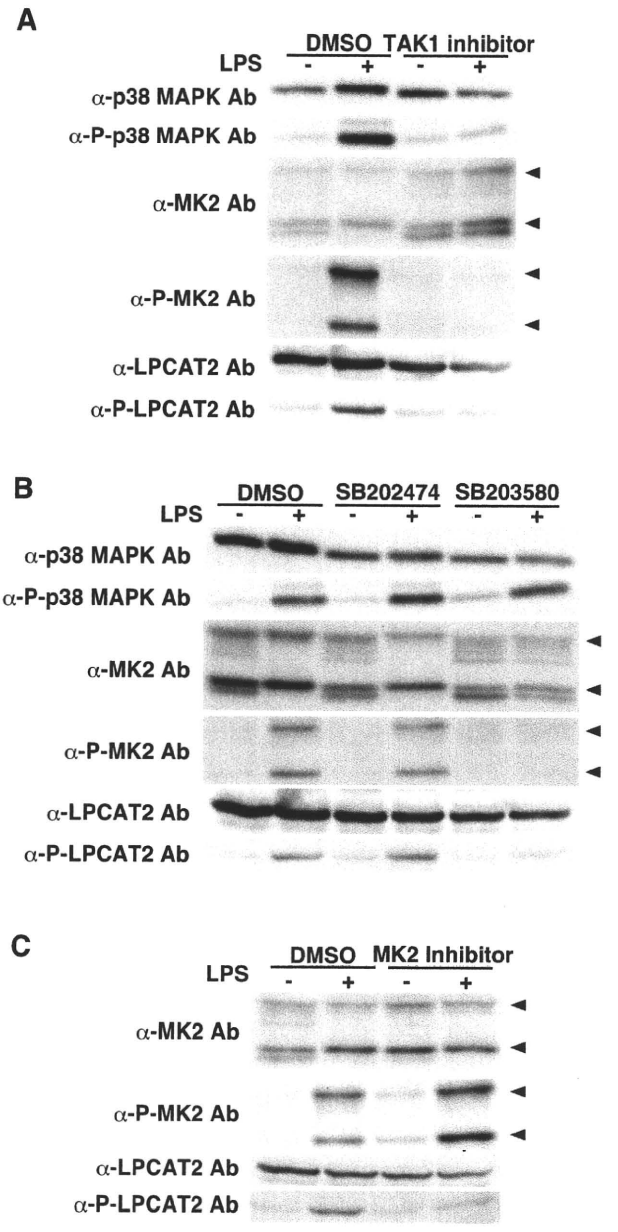
A
DMSO
TAK1 inhibitor
LPS
- + - +
α-p38 MAPK Ab
α-P-p38 MAPK Ab
α-MK2 Ab
α-P-MK2 Ab
α-LPCAT2 Ab
α-P-LPCAT2 Ab
B
DMSO
SB202474
SB203580
LPS
- + - + - +
α-p38 MAPK Ab
α-P-p38 MAPK Ab
α-MK2 Ab
α-P-MK2 Ab
α-LPCAT2 Ab
α-P-LPCAT2 Ab
C
DMSO
MK2 Inhibitor
LPS
- + - +
α-MK2 Ab
α-P-MK2 Ab
α-LPCAT2 Ab
α-P-LPCAT2 Ab

Fig. 5

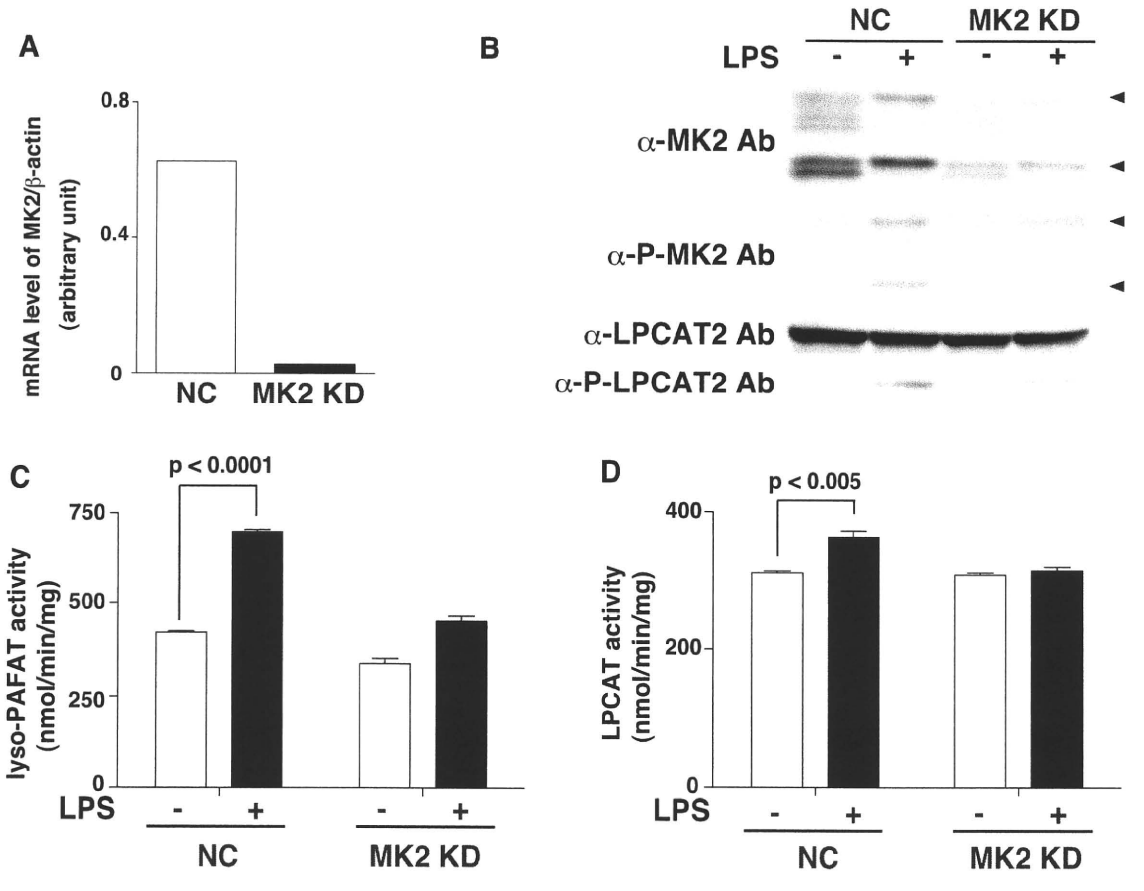
A
mRNA level of MK2/β-actin (arbitrary unit)
0.8
0.4
0
NC
MK2 KD
B
NC
MK2 KD
LPS
- + - +
α-MK2 Ab
α-P-MK2 Ab
α-LPCAT2 Ab
α-P-LPCAT2 Ab
C
p < 0.0001
lyso-PAFAT activity (nmol/min/mg)
750
500
250
0
LPS
- + - +
NC
MK2 KD
D
p < 0.005
LPCAT activity (nmol/min/mg)
400
200
0
LPS
- + - +
NC
MK2 KD

Fig. 6

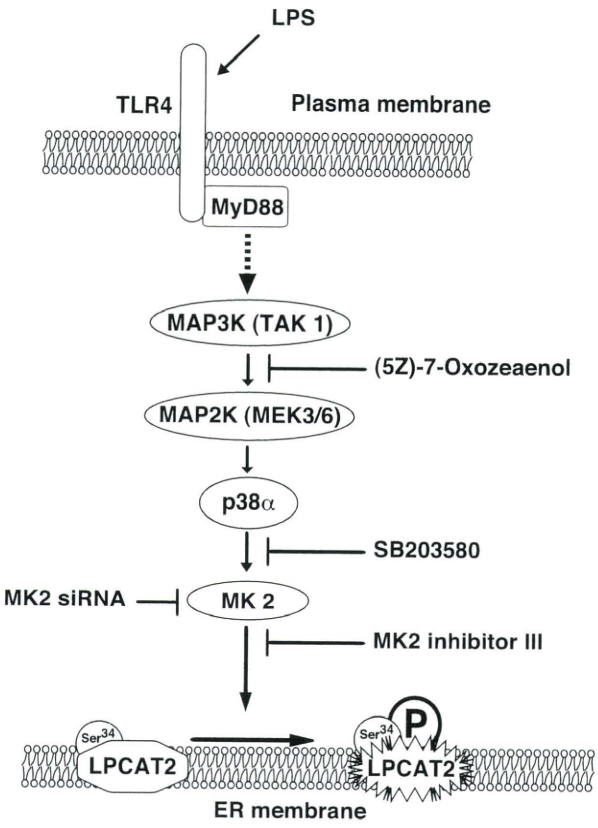
LPS
TLR4
Plasma membrane
MyD88
MAP3K (TAK 1)
(5Z)-7-Oxozeaenol
MAP2K (MEK3/6)
p38α
SB203580
MK2 siRNA
MK 2
MK2 inhibitor III
Ser34
P
LPCAT2
LPCAT2
ER membrane

Role of lysophosphatidic acid acyltransferase 3 for the supply of highly polyunsaturated fatty acids in TM4 sertoli cells

Andreas Koeberle, Hideo Shindou[1], Takeshi Harayama and Takao Shimizu

Department of Biochemistry and Molecular Biology, Faculty of Medicine, The University of Tokyo, Tokyo, Japan

[1] Correspondence: Hideo Shindou, Department of Biochemistry and Molecular Biology, Faculty of Medicine, The University of Tokyo, Bunkyo-ku, Tokyo, 113-0033, Japan. Tel: +81-3-5802-2925; Fax: +81-3-3813-8732; E-mail: hshindou-tky@umin.ac.jp

Short title: LPAAT3 in lipid homeostasis of Sertoli cells

Abstract

Sertoli cells supply germ cells with nutrients including highly polyunsaturated fatty acids (hPUFAs) which are essential for testicular function. We have previously reported high expression of lysophosphatidic acid acyltransferase (LPAAT)3 in mature mouse testis and suggested an arachidonoyl-transferase activity to LPA. To investigate the role of LPAAT3 in the storage and release of PUFAs, TM4 Sertoli cells were stably transfected with LPAAT3-small hairpin (sh)RNA. Arachidonoyl-, eicosapentaenoyl-, and docosapentaenoyl-containing phosphatidylcholine (PC) and linoleoyl-containing phosphatidylethanolamine (PE), phosphatidylserine (PS) and phosphatidylglycerol were significantly decreased as determined by liquid chromatography coupled to electrospray ionization mass spectrometry. Expression of murine LPAAT3 in Chinese hamster ovary (CHO)-K1 cells had essentially an opposite effect. The level of polyunsaturated PC correlated with cellular levels of free docosapentaenoic acid and eicosapentaenoic acid in TM4 and CHO-K1 cells, respectively. Activity assays using microsomal preparations as source of LPAAT3 revealed an excessive PA synthesis from LPA acceptors for docosahexaenoyl-, arachidonoyl- and less pronounced for linoleoyl-CoA. We propose that the efficient incorporation of hPUFAs into PA - the precursor of several phospholipids including PC - and the selective increase of the poly-unsaturated PC pool in TM4 Sertoli cells might be required for the controlled release of hPUFAs and their supply to germ cells.

Key Words: 1-acylglycerol-3-phosphate O-acyltransferase, phosphatidylcholine, phosphatidic acid, testis

Introduction

Sertoli cells form as a structural element of the seminiferous epithelium the blood-testis barrier and supply developing germ cells with nutrients, mitogens and differentiation factors (1). A crucial role of the number and functionality of Sertoli cells for spermatogenesis is well established (2). Long chain polyunsaturated fatty acids (PUFAs, n-6 and n-3), which form 8-24% of the fatty acids of human testis (3) and up to 58% in human semen (4), were early recognized to be critical for fertility. They accumulate particularly in germ cells (5, 6), although Sertoli cells show a considerable more efficient synthesis of docosapentaenoic acid (n-6, 22:5) and docosahexaenoic acid (n-3, 22:6) (7-12). This led to the experimentally unconfirmed hypothesis of a transport of PUFAs from Sertoli cells to germ cells (7, 8, 13, 14). Accordingly, fatty acid desaturases (Δ5- and Δ6-desaturase, SCD1 and SCD2), which are required for the biosynthesis of PUFAs, were found to be preliminarily localized in Sertoli cells and show only minor expression in germ cells (15). In crude testicular cells as well as in isolated germ cells, exogenously added PUFAs are preferentially incorporated into phosphatidylcholine (PC) compared to other phospholipid (PL) subgroups (8). However, although the PL and fatty acid composition of testis is well established (16-18), a complete lipidomic analysis of neither Sertoli cells nor testis has been performed, the involved acyltransferases have not been investigated, and also a functional relationship between PL incorporation and release of PUFAs is still elusive.

Lysophosphatidic acid acyltransferases (LPAATs) esterify the *sn*-2 position of lyso-phosphatidic acid (lyso-PA) using acyl-CoAs as substrate (for review see (19)). They are required for the *de novo* synthesis of PA as precursor of other glycero-PLs. At least three LPAATs have been identified and cloned so far. They considerably differ in their tissue distribution and their substrate specificity. Human LPAAT1 is ubiquitously expressed (20, 21), and also human LPAAT2 is found in most tissues with highest expression levels in heart,

liver and adipocytes (20, 22). In contrast, mouse LPAAT3 is mainly localized in testis, although lower mRNA expression levels can be found for many other tissues, too (e.g., for kidney, heart, epididymis) (23). We have recently shown a preference of LPAAT3 for arachidonoyl (20:4)-CoA as acyl-donor substrate over palmitoyl (16:0)-, oleoyl (n-9, 18:1)- and linoleoyl (n-6, 18:2)-CoA using microsomes from mLPAAT3-overexpressing Chinese hamster ovary (CHO)-K1 cells (23). Moreover, we revealed *in vitro* lysophosphatidylinositol acyltransferase (LPIAT) activity for LPAAT3 again with preference for 20:4-CoA (23). The cellular and *in vivo* functions of LPAAT3 are less defined. Recently, a role of LPAAT3 in regulating Golgi structure and membrane trafficking was elucidated (24), and we could show a strong upregulation of LPAAT3 mRNA and protein expression during murine testis maturation which might at least partly be ascribed to the induction of LPAAT3 in Sertoli cells by estradiol (23). However, the consequences of LPAAT3 expression for testis function are still elusive. Here, we present for the first time a lipidomic approach investigating the molecular PL composition of a Sertoli cell line. LPAAT3 was found to determine the cellular levels of polyunsaturated PC whose abundance correlates with the release of specific highly polyunsaturated fatty acids (hPUFAs). We suggest that LPAAT3 provides a membrane pool of PC with hPUFAs in *sn*-2 position thus allowing their controlled supply to germ cells.

Materials and Methods

Reagents

DMEM, F12-HAM, trypsin/EDTA solution and quantitative real time-PCR primers were obtained from Sigma-Aldrich (St. Louis, MO, USA). 1,2-Di-myristoyl-(14:0)-*sn*-glycero-3-PC and 1,2-di-14:0-*sn*-glycero-3-phosphatidylethanolamine (-PE) standards were purchased from NOF corporation (Tokyo, Japan). All other PL standards, lyso-PLs and acyl-CoAs were obtained from Avanti Polar Lipids (Alabaster, AL, USA). Lipids were dissolved in 50-75% ethanol (aqueous) and stored at -30°C. Materials used: EDTA, Dojindo Molecular Technologies (Tokyo, Japan); fetal bovine serum, geneticin, Lipofectamin 2000, Invitrogen (Carlsbad, CA, USA); sodium dodecyl sulfate, Nacalai Tesque Inc. (Kyoto, Japan); skim milk, BD Diagnostic Systems (Sparks, MD, USA). Solvents and all other chemicals were obtained from Wako Pure Chemicals (Osaka, Japan) unless stated otherwise.

Cells

Murine TM4 Sertoli cells and CHO-K1 cells were cultured at 37°C in a 5% CO_2 incubator in F12-HAM/DMEM (1:1, v/v) medium containing 5% (v/v) heat-inactivated horse serum and 2.5% (v/v) fetal bovine serum or F12-HAM medium supplemented with 10% (v/v) fetal bovine serum, respectively. After 3 days, confluent cells were detached using 1 × trypsin/EDTA solution and reseeded at 6×10^5 cells in 10 ml medium in 10 cm culture dishes. For TM4 cells, stable transfected with vector- or mLPAAT3-small hairpin (sh)RNA, the culture medium was supplemented with a maintenance concentration of geneticin (0.375 mg/ml).

Knockdown of mLPAAT3 in TM4 Sertoli cells

SureSilencing™ shRNA plasmids containing shRNA sequences under the control of the U1 promotor and a neomycin resistance marker were obtained from SA Biosciences (Frederick, MD, USA). Target sites in mouse LPAAT3 mRNA were 5'-GAAGGAGCATGTGGTTGTT-AT-3' (lot 1), 5'-GTACAAGCAGAAGGGTGTATT-3' (lot 2), 5'-AGCTGACTACCCAGA-GTACAT-3' (lot 3) and 5'-GGATCCTGTATGGGAAGAAAT-3' (lot 4). The negative control-shRNA plasmid encoded for the non-matching sequence 5'-GGAATCTCATTCGAT-GCATAC-3'. TM4 cells (5×10^5 cells/well) cultured in 6-well plates (Corning, New York, NY, USA) were transfected with 4 μg of the above constructs using Lipofectamine 2000 according to the manufacturer's instructions. After 48 h at 37°C and 5% CO_2, cells were selected with 0.7 mg/ml geneticin for 1 week before changing to the maintenance concentration (0.375 mg/ml geneticin, polyclonal 'lot 3'-shRNA transfected cells). Single cell clones were selected and expanded only for 'lot 3'-shRNA transfected cells (monoclonal 'lot 3'-shRNA transfected cells, see below).

Expression of FLAG/mLPAAT3 in Chinese hamster ovary-K1 cells

Transfection of CHO-K1 cells was performed according to (23). In brief, CHO-K1 cells were seeded onto 10 cm dishes at a density of 2.7×10^6 cells/10 cm dish 24 h before transfection. pCXN2.1 vector or FLAG/mLPAAT3-pCXN2.1 (12 μg, each) (23) was transfected using Lipofectamine 2000 according to the manufacturer's instructions. At 48 h after transfection, cells were trypsinized for lipid extraction and PL analysis or were used for the preparation of microsomes.

Preparation of microsomes from TM4 and CHO-K1 cells

Cells (10 cm dish, confluent) were scraped into 1 ml of ice-cold buffer containing 20 mM Tris-HCl (pH 7.4), 300 mM sucrose and a proteinase inhibitor cocktail Complete (Roche Applied Science, Basel, Switzerland) for the preparation of microsomes. After sonification of

the cells on ice (3 × 30 s), the lysate was subjected to differential centrifugation at 9,000 × g for 15 min and 100,000 × g for 1 h at 4°C. Pellets were suspended in buffer containing 20 mM Tris-HCl (pH 7.4), 300 mM sucrose and 1 mM EDTA, and the total protein concentration was determined.

Quantitative real-time PCR

Total RNA was prepared using the RNeasy Mini Kit (Qiagen, Valencia, CA, USA), and first-strand cDNAs were synthesized using Superscript III (Invitrogen, Carlsbad, CA, USA). PCR (LightCycler System, Roche Applied Science, Basel, Switzerland) was conducted in microcapillary tubes containing 2 µl cDNA solution, 1 × FastStart DNA Master SYBR Green I (Roche Applied Science, Basel, Switzerland), and 0.5 mM of each of sense and anti-sense primers (reaction volume of 20 µl, see Table 1 for primer sequences). Denaturation was performed at 95°C for 3 min. The 45 cycles of amplification consisted of denaturation at 95°C for 15 s, annealing at 65°C for 5 s, and extension at 72°C for 7 s. cDNA levels were quantified using the second derivative maximum method of the LightCycler analysis software. Results, given as percentage of control, were normalized to the glyceroaldehyde-3-phosphate-dehydrogenase (GAPDH) mRNA levels. mRNA expression levels in amol/µg of total RNA were calculated using standard curves of pCXN2.1 vectors encoding FLAG/mLPAAT-1 (23), -2 (see supplemental data for cloning) and -3 (23).

Western blot

Microsomes (100,000 × g pellets, 5 µg) in 1 × sample loading buffer (25 mM Tris-HCl pH 6.5, 5% (v/v) sucrose, 1% (m/v) sodium dodecyl sulfate (SDS), 0.05% (m/v) bromophenol blue) were resolved by 10% (m/v) SDS-PAGE and transferred to a Hybond ECL nitro-cellulose membrane (GE Healthcare, Chalfont St. Giles, UK). After blocking with 5% (m/v)

skim milk overnight at 4°C, membranes were washed and incubated with anti-FLAG M2 monoclonal antibody (IBI-Kodak, Rochester, NY, USA, 1:1000) for 2 h at room temperature. The membranes were washed again, incubated with horseradish-peroxidase-labeled anti-mouse IgG (GE Healthcare, Chalfont St. Giles, UK, 1:1000) for 2 h at room temperature and exposed to ECL reagents (GE Healthcare, Chalfont St. Giles, UK). Immunoreactive bands were visualized by a Luminescent Image Analyzer (Fujifilm Life Science, Tokyo, Japan).

Extraction of PLs and sample pre-treatment for LC-MS and LC-MS/MS

Cationic PLs (PC and PE) from cultured cells (1×10^6) and PLs from *in vitro* activity assays were extracted according to the method of Bligh and Dyer (25). 1,2-Di-14:0-*sn*-glycero-3-PC and 1,2-di-14:0-*sn*-glycero-3-PE were used as internal standard for lipidomic studies (2 nmol, each). The extracted lipids were solved in 100 µl methanol, diluted and applied to liquid chromatography tandem mass spectrometry (LC-MS/MS) analysis.

Anionic PLs (phosphatidylserine (PS), phosphatidylinositol (PI), phosphatidylglycerol (PG) and PA) and free fatty acids from cultured cells (1×10^6) were extracted by *n*-butanol (500 µl) from an aqueous phase (500 µl), and the *n*-butanol extract was mixed with 0.5 ml methanol/chloroform (1:1, v/v). 1,2-Di-14:0-*sn*-glycero-3-PS and 1,2-di-14:0-*sn*-glycero-3-PG were used as internal standards (0.75 nmol each). To enrich anionic PLs and fatty acids and to avoid matrix effects, they were separated by anion exchange chromatography according to (26). In brief, the sample (1 ml in *n*-butanol/methanol/chloroform = 2:1:1, v/v/v) was applied to a column containing activated and equilibrated DEAE cellulose (750 µl). The column was washed with chloroform/methanol (1:1, v/v), and bound PLs were eluted with chloroform/methanol/28% aqueous ammonia/28% acetic acid (200:100:3:0.9, v/v/v/v). The eluates were dried under vacuum and redissolved in 100 µl methanol. Diluted aliquots were used for LC-MS or LC-MS/MS analysis.